Solvation effects on molecular pure radiative lifetime and absorption oscillator strength in clusters

Abraham Penner, Aviv Amirav, Joshua Jortner, and Abraham Nitzan
School of Chemistry, Sackler Faculty of Exact Sciences, Tel Aviv University, 69 978 Tel-Aviv, Israel

Joel Gersten
Department of Physics, City College of the City University of New York, New York, New York 10031

(Received 16 November 1989; accepted 5 January 1990)

The solvation effects on the molecular pure radiative lifetime, its absorption line shape, oscillator strength, and spectral red shift are studied for 9, 10-dichloranthracene embedded in clusters of argon, krypton, and xenon. The clusters are synthesized in a supersonic free-jet coexpansion of the organic molecule with the rare gas. Cluster size is controlled by the nozzle backing pressure and its pure radiative lifetime is obtained by measuring both the fluorescence lifetime and the absolute emission quantum yield. For small (jet atom) clusters the pure radiative lifetime is increased by subsequently adding rare gas atoms. For up to two rare gas atoms this increase correlates with the atomic polarizabilities and with the spectral red shift. For Ar and Kr this trend of increasing radiative lifetime continues up to clusters of six rare gas atoms. These results are in good agreement with calculations based on classical electromagnetic theory using point polarizable dipoles for the atom and a simplified charge distribution for the molecule. For large clusters of Ar (up to ~ 1000 atoms) both the spectral red shift and the lifetime become cluster size independent. This is also in agreement with classical electromagnetic theory using a model of a point (molecular) dipole embedded in a dielectric (rare gas) sphere. Both experiment and theory indicate that the radiative lifetime in this limit is still larger than that of the free molecule, which in itself is longer than that expected in the bulk solvent. This implies that a further cluster size evolution of this quantity is expected upon increasing the cluster size above the radiation wavelength. We also report on a sudden lineshape broadening and a slight spectral blue shift that accompanies the growth of large molecule–argon clusters and which we interpret as originating from a possible transition towards the surface of the molecule in order to minimize growth strain.

I. INTRODUCTION

This research addresses several questions concerning the transition from isolated to matrix isolated molecules. Specifically we focus on optical properties (the solvent spectral shift $\Delta\omega$ and the solvent affected pure radiative lifetime τ_r) of molecules solvated in rare gas clusters and on the cluster size evolution of these properties. In a previous paper[1] we found that the τ_r of 9, 10-dichloranthracene (9, 10-DCA) in small Ar clusters is larger by $\sim 5\%$ from τ_r of the free (isolated) molecule. In contrast, theory and experimental measurements (in cyclohexane) tell us that the radiative lifetime of 9, 10-DCA in bulk solvent is about half that of the free molecule. This shows the unique features of the cluster environment and lead us to expect a nontrivial cluster size evolution.

Other issues associated with this study are as follows: (a) What are the basic physical parameters and interaction that govern the solvent effect on τ_r and on $\Delta\omega$? (b) Is the relationship between τ_r and oscillator strength (integrated absorption) solvent dependent? Is it cluster size dependent? (c) How do structural details in the finite cluster affect τ_r and $\Delta\omega$? (d) At what size of the finite cluster do solvation effects saturate at their bulk solvent values? (e) Is the classical electromagnetic theory adequate for a theoretical treatment of these phenomena?

In our previous paper we have argued that classical electrodynamics is sufficient for discussing such issues as long as we limit ourselves to linear near-resonance optical phenomena. We use this classical framework to discuss the other issues listed above. We present more detailed experimental and theoretical results and show that the theory, within the simple model adopted here, can account semiquantitatively for the experimental observations. Remaining deviations are most probably associated with our lack of detailed knowledge of the cluster structure and of the molecular charge distribution.

The experimental work described below involves a measurement of the molecular fluorescence decay time τ and emission quantum yield Y (which together yield the pure radiative decay time $\tau_r = \tau/Y$) and of the absorption lineshape. 9, 10-dichloranthracene was studied by us extensively in the past and was chosen for this research because of its unique photophysical properties, as detailed below.

II. PHOTOPHYSICS OF 9, 10-DICHLORANTHRACENE

We have chosen 9, 10-DCA for this research for the very specific reason that it has an emission quantum yield of unity from the origin of S_1.[2,3] In 9, 10-DCA the origin of the second triplet lies above the origin of S_1[4] and thus the rate of intersystem crossing is very small and it does not exhibit an

 0021-9606/90/130147-12$03.00

external heavy atom effect upon complexing with xenon. The phosphorescence quantum yield in matrices was found to be smaller than 10^{-3}.[3,5] On the other hand, its singlet origin is high enough in its energy so that the rate of internal conversion is also very small.[6] For these two reasons the emission quantum yield of its singlet origin is very close to unity.

As emission quantum yields are hard to measure with precision better than 5%, and in our experimental setup we cannot measure Y for large clusters due to synthesis problems, we have chosen 9, 10-DCA, for which the measurement of the lifetime represents the true measurement of the pure radiative lifetime, unperturbed by solvation. Therefore, in this study we have measured the emission quantum yield only for small clusters of 9, 10-DCA with one or two Ar, Kr, or Xe atoms which is 1.00 ± 0.05 for all these clusters.[4] For larger clusters we have measured only lifetimes, and we believe they represent the true τ_r. In the worst case they always constitute a lower limit of τ_r.

III. EXPERIMENTAL

The basic elements of our experimental apparatus are described elsewhere[4] so that only the unique elements of this experiment will be outlined. We have used four different nozzles for the synthesis of 9, 10-DCA clusters with Ar, Kr, and Xe rare gases.

(a) A small 20 μ diameter platinum nozzle (electron microscope pinhole of Polaron company) could hold up to over 100 atm without overloading our 4 in. diffusion pump (Varian VHS 4).

(b) A pulsed slit nozzle[4] was used mostly for the absorption and quantum yield measurements but also for the lifetime measurements of small clusters up to 11 rare gas atoms.

(c) A conventional 150 μ stainless steel nozzle was used in a rotary pump alone mode of operation. It was successfully operated in the past for the generation of large clusters of tetracene, pentacene and anthracene with rare gases.[7-9]

(d) A 100 μ conical nozzle gave the highest cluster size at a given backing pressure (up to 100 atm) but with the broadest cluster size distribution function width. It was also used in the rotary pump alone mode of operation.[7] The nozzle backing pressures were regulated either by a needle valve, or by a Matheson high pressure regulator. A sample of 9, 10-DCA was heated behind the nozzle in the range 140–200 °C and mixed there with the carrier rare gases before expansion. An excimer pumped dye laser (Lambda Physik EMG53-MSC + FL2002E) crossed the supersonic free-jet expansion 4–5 mm downstream, and the fluorescence was focused into a photomultiplier (Hammamatsu-R1398) with a nominal 2 ns risetime. The fluorescence was processed using a LeCroy 9400 signal averager and fed into an IBM-PC. The decay curves obtained were fitted to an exponential decay using a least mean square fit which was biased to the square root of the signal height so that the higher signal was given a higher statistical weight. In order to minimize errors and to obtain ± 0.2 ns precision we had to minimize RF interferences caused by the laser to below 0.5 mv by appropriate shielding and grounding. In addition, we had to operate the photomultiplier always at the same voltage and to control the laser output by its variable attenuation so that we had the same initial decay signal height. A trigger was obtained from the RF of the laser firing. In Fig. 1 we show typical results obtained from 9, 10-DCA and its clusters. Each decay curve was taken as the average of about a thousand laser shots and each measurement was the average of at least six decays as in Fig. 1. These measurements were rechecked using several nozzles and on several working days. For these reasons we estimate our relative precision to be ± 0.2 ns. The absolute accuracy is probably determined by the LeCroy digitizer and our estimated value for that is ± 2 ns. The absorption spectra and emission quantum yield measurements were determined as previously described,[2,4] using our pulsed slit nozzle and pulsed simmered short arc xenon lamp followed by a monochromator. The details of cluster growth dynamics are given elsewhere.[7-9]

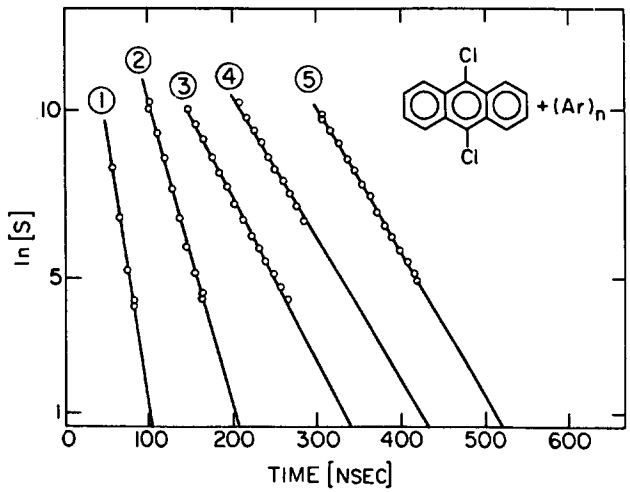

FIG. 1. Time resolved emission of 9,10-dichloroanthracene and its complexes with argon. The decays were processed 20 ns after the peak at 10 ns intervals. The solid lines are of a computer least mean square fit. In all cases over six such decays were averaged to give a single measurement. The decays numbered 1–5 are: (1) Laser stray light. (2) 400 cm^{-1} vibration of 9, 10-DCA. (3) Electronic orgin of 9, 10-DCA. (4) 9, 10-DCA$(Ar)_2$. (5) Large cluster of 9, 10-DCA$(Ar)_n$ with saturated red shift.

IV. EXPERIMENTAL RESULTS

A. The spectra of small clusters

In Fig. 2 we show the argon pressure dependence of 9, 10-DCA$(Ar)_n$ clusters, for small clusters of up to $n = 7$. The size assignment of these clusters is according to their argon pressure dependence and it follows their order of red shift so that the first peak is from the bare molecule, the second one is from 9, 10-DCA$(Ar)_1$, the third one is from 9, 10-DCA$(Ar)_2$ and so on.[8,10] From the added red shift per added atom it was concluded that their structure is as follows[10]: The first cluster has its argon above the center aromatic ring. In 9, 10-DCA$(Ar)_2$ the structure is of a sandwich type on the center aromatic ring. In 9, 10-DCA$(Ar)_3$ two atoms are on one side and one on the other side and the fourth argon atom is added to form a triplet on one side, one on each ring and one atom on the other side, and only then,

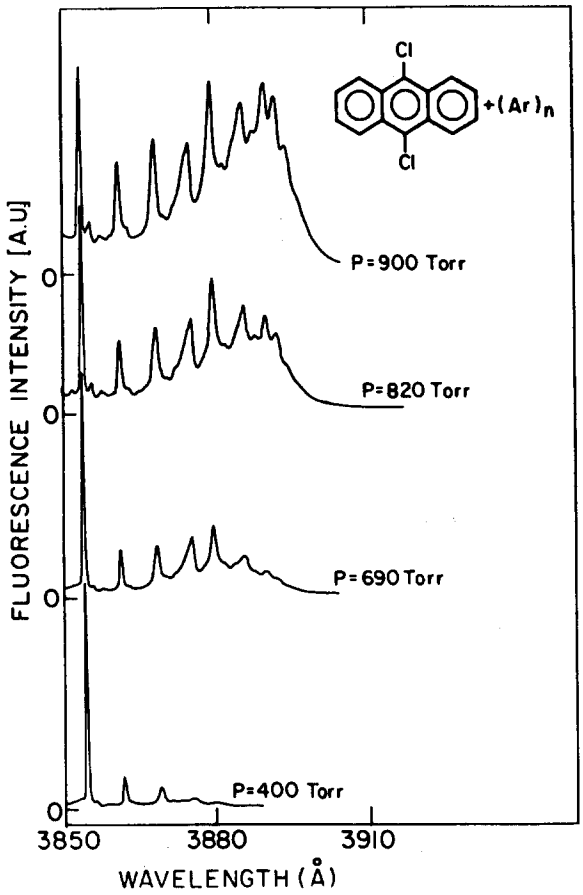

FIG. 2. The argon backing pressure effect on the generation of 9, 10-dichloroanthracene complexes with argon. The nozzle diameter was 20 μ and its temperature was 160 °C.

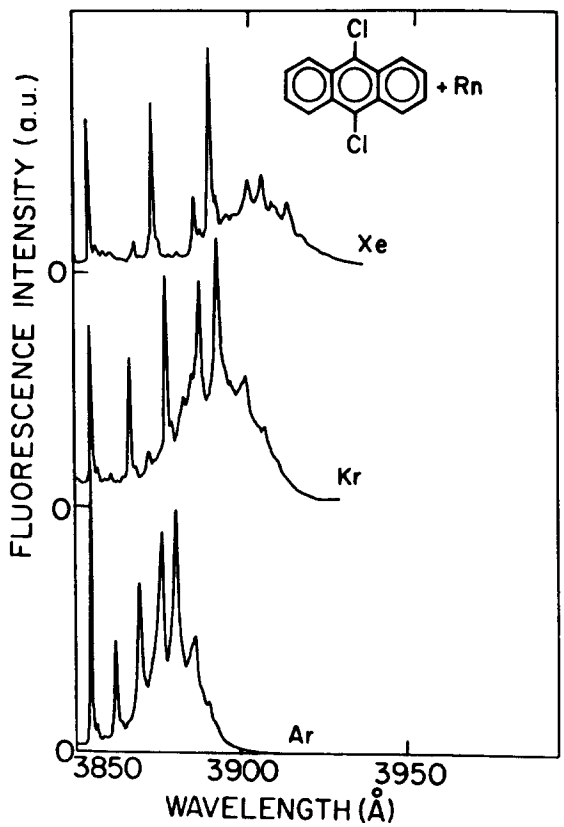

FIG. 3. Rare-gas complexes of 9, 10-DCA. The nozzle diameter was 20 μ and its temperature was 170 °C. The argon, krypton and xenon backing pressures were 800, 600, and 300 Torr respectively.

the fifth and sixth atoms are put on the other side. The conclusion from that analysis[10] is that the first six atoms are all situated above the plan of the transition dipole moment and qualitatively are expected to increase the pure radiative lifetime.[1]

In Fig. 3 we show the spectra of small clusters of 9, 10-DCA with argon, krypton, and xenon rare gases which are very analogous to other spectra of such complexes.[8] Again the small clusters exhibit a well defined spectral feature which is amenable for study of both its lifetime and emission quantum yield.

B. The pure radiative lifetime of small clusters

In Fig. 4 we plot both the spectral red shift and the added relative pure radiative lifetime versus the rare-gas polarizability. In all our measurements we found an increase of the pure radiative lifetime upon complexing with argon, krypton or xenon. The important observation, however, is that this increase of τ_r could well be correlated with the rare-gas polarizability. On the other hand, it is well established that the spectral red shift correlates well with the rare-gas polarizability[11] as is also demonstrated again for our system in Fig. 4. This result implies that the change in τ_r correlates with the spectral red shift and suggests that both of them originate from dispersive interactions as was suggested earlier.[1] We also note that the same relationship holds for the second added rare-gas atom where both the added spectral red shift and the added τ_r linearly increased with the atomic polarizability.

Another important piece of information found in Fig. 4 pertains to nonradiative processes in 9, 10-DCA. As was elaborated elsewhere[4] 9, 10-DCA does not exhibit an external heavy atom effect due to the energetic location of its T_2 above S_1 and the resulting lack of mediated intersystem crossing. From our point of view, the lack of an external heavy atom effect on both complexes, 9, 10-DCA(Xe) and 9, 10-DCA$(Xe)_2$ and the observation that in molecules, where it exists, this effect saturates on the addition of the first atom,[12] strongly suggest that our complexes with the much lighter argon atoms are totally immune against solvation effects on the nonradiative intersystem crossing rates, which already are much smaller than the radiative rate in 9, 10-DCA. Thus for clusters with more than two rare-gas atoms, we have measured the lifetime alone, and accepted it as τ_r or at least as a lower limit for it. We note again that the data in Fig. 4 represents the true τ_r as the measured emission quantum yields for these clusters was 1.00 ± 0.05.[4]

In Fig. 5 we plot the emission lifetime of 9, 10-DCA$(Ar)_n$, where $n = 0$–8, against the spectral red shift. It is clearly observed that the lifetime increases with the num-

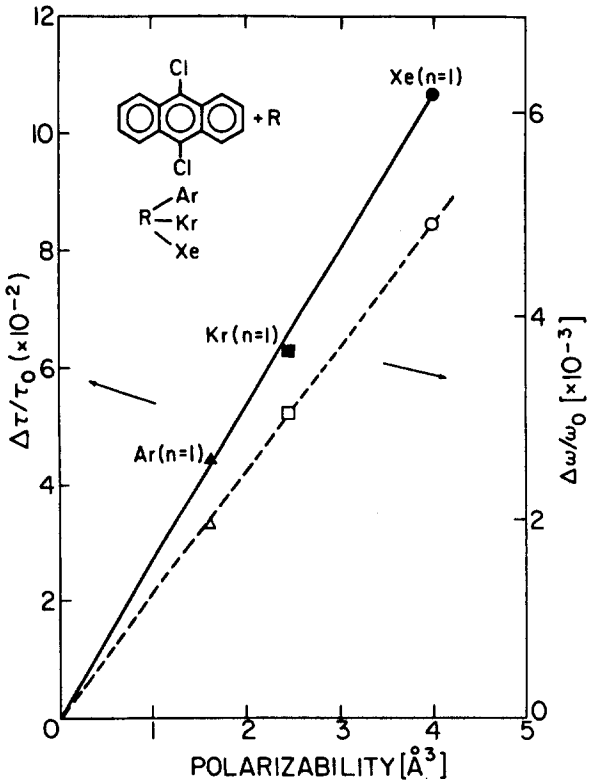

FIG. 4. The added pure radiative lifetime and the spectral red shift of argon, krypton, and xenon van der Waals complexes with 9, 10-dichloroanthracene against the rare-gas atom polarizabilities.

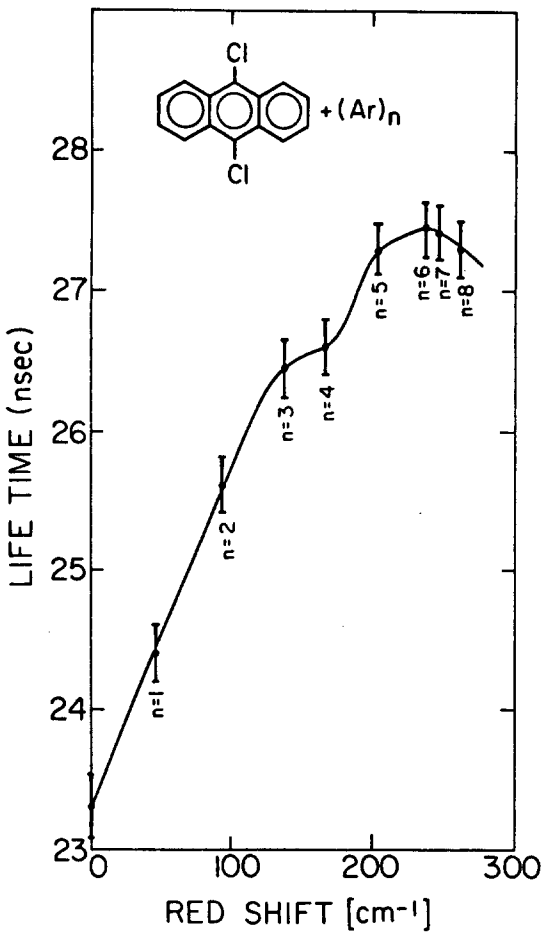

FIG. 5. The pure radiative lifetime of several 9, 10-DCA(Ar)$_n$ complexes (n-number of argon atoms) vs their spectral red shift.

ber of argon atoms up to $n = 6$, which is in full agreement with the qualitative theoretical prediction[1] based on our proposed structure[10] of these six argons being above and below the aromatic rings and thus perpendicular to the transition dipole moment.

We also observe in Fig. 5 that the linear relationship between τ_r and the spectral red shift is degraded for $n > 2$. This is related to the different atom position dependence of these two observables as discussed in Sec. V. A very similar behavior was also observed in 9, 10-DCA(Kr)$_n$ for the krypton clusters with $n = 0$–6.

C. Large clusters and their pure radiative lifetime

In Fig. 6 we show the spectra of 9, 10-DCA(Ar)$_n$ and its dependence on the argon backing pressure. As the argon backing pressure was raised the average cluster size was correspondingly increased. A rough measure of the mean cluster size under our experimental conditions can be inferred from the mass resolved spectra for 9, 10-DCA(Ar)$_n$ clusters obtained by Even *et al.*[13] By the comparison of the spectral shift of the band maximum (Fig. 6) with the spectral shift for the mass selected clusters[13] we infer that the spectral shift for the $n = 54$ cluster $\Delta\nu = 535$ cm^{-1} corresponds under the experimental conditions of Fig. 6 to $p \simeq 18$ atm. The cluster growth kinetics at moderate and high stagnation pressure p implies that $\langle n\rangle \propto p^{\beta}$ with $\beta = 1$–2. One expects that $\alpha = 2$ at low p ($\langle n\rangle \lesssim 10$) as appropriate for three-body collisions, $\beta \simeq 1$ at higher p where cluster growth is stabilized by evaporation, while at high p values β increases from the value of unity due to the contribution of intercluster collisions. Utilizing the value of $\langle n\rangle = 54$ at $p = 18$ atm, the higher pressure of 100 atm and 20 μ nozzle diameter we estimate for the cluster size an upper limit of $\langle n\rangle = 1500$ (with $\beta = 2$) and a lower limit of $\langle n\rangle \simeq 300$ (with $\beta = 1$), thus concluding that the largest cluster synthesized with the 20 μ nozzle is $\langle n\rangle = 10^3$ with an uncertainty of $\pm$ 50%. The mean cluster size synthesized with the 100 μ conical nozzle is estimated to be much larger than 10^3.

In Fig. 7 we plot the lifetime of the clusters vs their spectral shifts. The lowest points correspond to well characterized clusters with $n = 1$–11, which could be spectrally identified, however, for $n > 4$ some spectral overlap occurs between clusters of adjacent n values. The spectral shift data for $n > 11$ correspond to the maxima of broad spectral bands, whose linewidth originates from inhomogeneous broadening due to the superposition of different cluster sizes, from distinct isomers of the same size, as well as to homogeneous broadening. The single point at $\Delta\nu = 592$ cm^{-1} represents a saturation in both the lifetime and the red spectral shift, which shows no further dependence on the cluster size. We

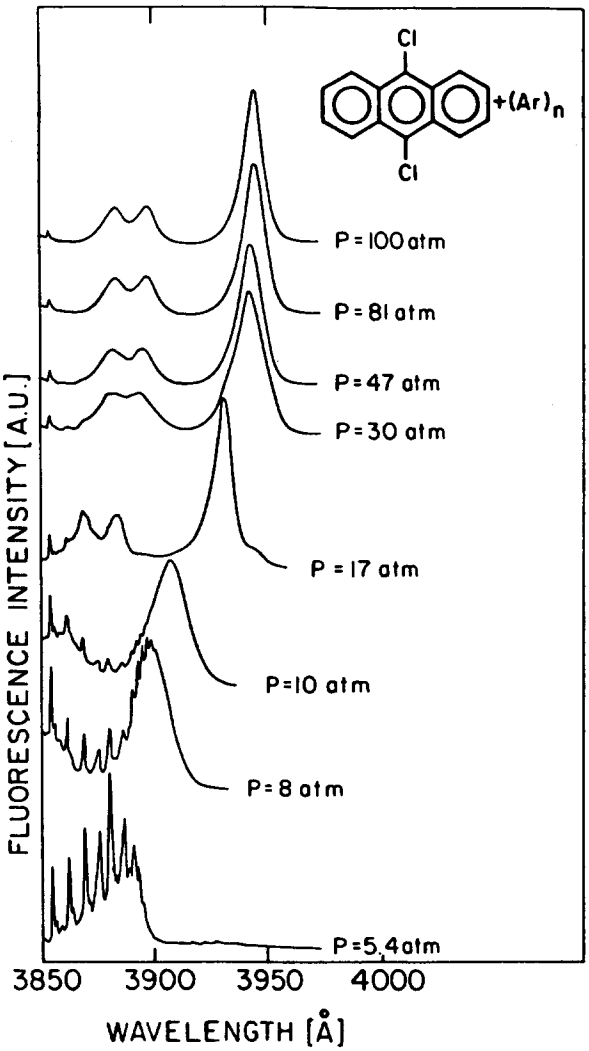

FIG. 6. The pressure effect on the spectroscopy of 9, 10-DCA clusters with argon. The nozzle diameter was 20 μ and its temperature was 190 °C.

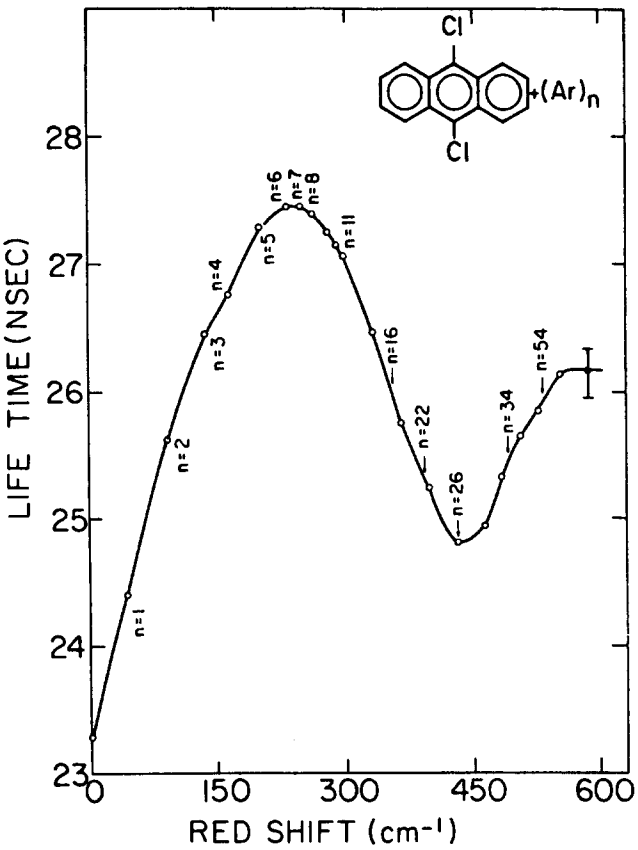

FIG. 7. The emission lifetime of argon complexes of 9, 10-DCA vs their spectral red shift. The spectral positions of the first eleven clusters are indicated. In each case the lifetime measurement was performed using several nozzles and at argon backing pressure where the yield of that cluster was optimized.

note in passing that the spectral shift constitutes a highly nonlinear measure of the cluster size. From the data of Fig. 7 we infer that τ_r increases up to $n = 6$ as is expected on the basis of the structural information which indicates that these Ar atoms are located above and below the aromatic ring. Subsequently τ_r starts to decrease for $n = 8$–26 with increasing n, as the first solvation layer is built on the sides of the 9, 10-DCA. The minimum of τ_r occurs for a red spectral shift of 435 cm^{-1}, which according to the mass resolved data[13] corresponds to $n = 26$. Above this cluster size τ_r starts to increase again. On the basis of theoretical considerations we assert that this increase of τ_r for $n > 26$ corresponds to the buildup of the second solvation layer. Thus the minimum of τ_r vs $\Delta\nu$ marks the completion of the first solvation shell. The value of $n = 26$ inferred from the τ_r data for the closure of the first solvation shell is close to but somewhat lower than the value of $n = 35$ inferred by Even *et al.*[13] for the saturation of the homogeneous line broadening in mass resolved 9, 10-DCA$(Ar)_n$ spectra. Further we note that for large clusters (above $\sim 10^2$) τ_r saturates at a value of 26.1 ns. It is important to note that the pure radiative lifetime saturates at the same cluster sizes as does the spectral red-shift, as is expected on the basis of the assumption that both these observables originate from polarizability interactions, as is also implied for Fig. 4.

D. The transition from isolated to matrix isolated molecule clusters and solvent

An important observation drawn from Fig. 7 is that for large clusters where the spectral red-shift saturates, the pure radiative lifetime also saturates at a value *larger* by 12% than that of the bare molecule. However the pure radiative lifetime of 9, 10-DCA was measured by Berlman[14] to be 15.4 ns in cyclohexane solution. We note that pure radiative lifetime reduction upon bulk solvation is also found for anthracene,[2] for which τ_r is 31 nsec in the bare molecule and 13.6 ns in cyclohexane,[14] and for tetracene whose τ_r is 50 ns for the bare molecule[2,15] and 30.5 ns in cyclohexane.[14]

In Fig. 8 we support the general notion that upon increasing the nozzle backing pressures, the clusters are still growing, even though the spectral red shift is saturated. For this purpose we have used a 100 μ conical nozzle which is much more efficient in inducing cluster growth than the 20 μ

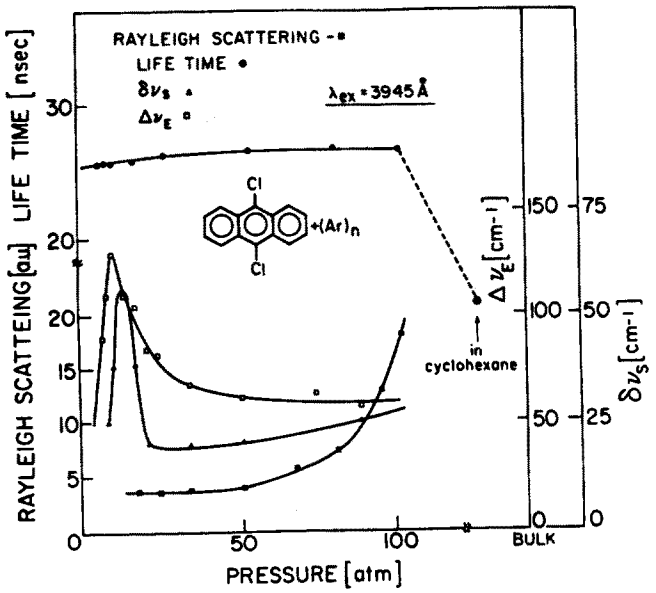

FIG. 8. Cluster growth after the saturation of their spectral red shift. The energy resolved emission width $\Delta\nu_E$(□□□) the emission Stokes shift $\delta\nu_S$(▲▲▲) the relative amount of Raleigh light scattering at 4000 Å(■■■) and the emission lifetime (●●●) of 9, 10-DCA embedded in large clusters of argon. A 150 μ conical nozzle was used at 180 °C. The experimental point in cyclohexane solution was taken from Ref. 4.

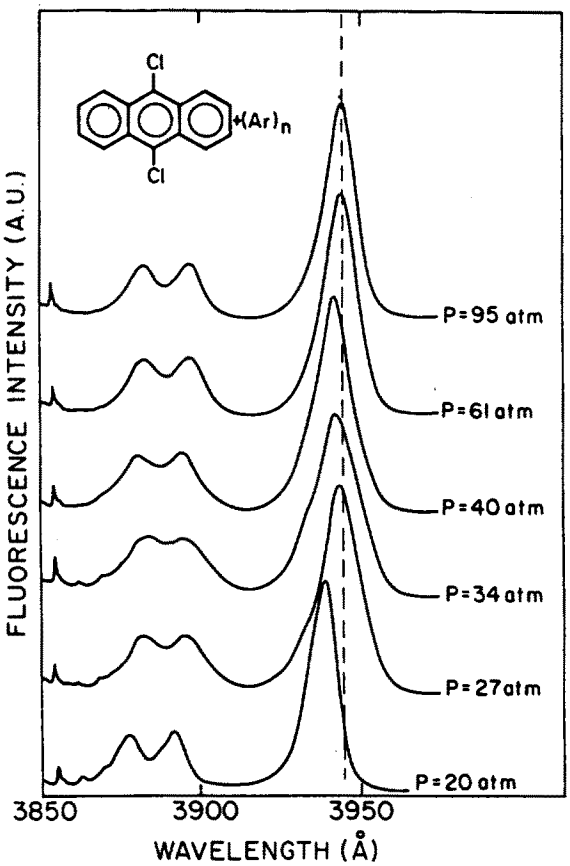

FIG. 9. Spectral manifestation of a structural change in 9, 10-DCA clusters with argon. The excitation spectra are plotted at the various indicated argon backing pressures. The dotted line is drawn to emphasize the slight blue shift at around 40 Atm. 20 μ nozzle diameter was used at 190 °C.

conventional nozzle and we plot the measured cluster lifetimes, the spectral width of the emission from the electronic origin, the Stokes shift of the energy resolved emission[10] and the amount of Rayleigh light scattering at a nonresonant wavelength of 4000 Å. From in increase in the Rayleigh light scattering as well as the pressure dependence of the emission width and its Stokes shift, we assert that the notion of cluster growth upon the increase of the argon backing pressure is further supported. We note that using the 100 μ conical nozzle, the spectral red shift, saturated at about 15 atm backing pressure. In spite of this, the measured lifetime remained practically constant at about 26 ns which is much longer than the solution value of τ_r. Further variations in τ_r (towards the bulk value) are therefore expected at much larger cluster sizes.

E. Transition in the cluster structure

One aspect that has been extensively discussed in the literature is isomerization or structural transitions in clusters.[16,17] While increasing the cluster size, upon the increase of the stagnation pressure, the spectral red shift saturates. In Fig. 9 we observe some peculiar features of the red spectral shift just before its saturation. In this range we observe that upon increasing p first a red shift then a blue shift (for $p = 27$–40 atm) and finally a red shift (for $p = 40$–95 atm) is exhibited.

In Fig. 10 we plot the p dependence of the spectral red shift, the excitation linewidth, the energy-resolved emission linewidth and the Stokes shift for the 20 μ nozzle. Similar results using other nozzles were obtained for different backing pressure scales. The first peak in the linewidth scale can be calibrated by comparison of our red shift values with those of the mass-resolved data,[13] to correspond to $\langle n\rangle = 22$–54. The widths of the cluster mass resolved spectra of Even *et al.*[13] in this size range are lower by a numerical factor of about 2 than our spectra, clearly reflecting the effects of inhomogeneous broadening. In this domain of relatively small cluster sizes the red shift per added atom is still relatively large as the first solvation layer is completed and around $n = 30$, whereupon the effects of cluster size distribution on the spectral shift are sizeable. The second peak in the excitation linewidth, emission linewidth and Stokes shift appears at large cluster sizes ($\langle n\rangle \geqslant 100$) where the first solvation layer is already completed and further solvation layers are built. This second peak correlates with the slight blue spectral shift (Fig. 10). A tentative interpretation of these observations involves the appearance of an asymmetric growth pattern of these large clusters, which coexist with symmetrical large clusters. Such coexistence will result in inhomogeneous line broadening and a slight blue spectral shift of the average excitation energy of these large clusters. Upon completion of the second shell at about 100 argon atoms, the argon–argon interaction starts to dominate over the argon-molecule interactions. To minimize strain the

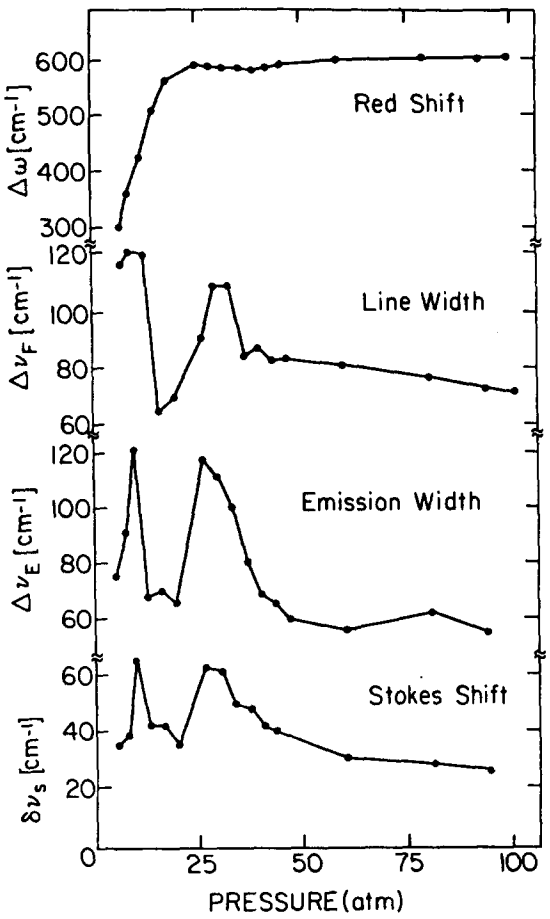

FIG. 10. The spectral red shift, excitation line width, emission line width and its Stokes shift of 9, 10-DCA clusters with argon against the nozzle backing pressure. Measurements are at the electronic origin as shown in Figs. 6 and 9. The nozzle diameter was 20 μ and its temperature was 190 °C.

cluster prefers to grow in an asymmetric way that can be viewed as a quasisurface molecule (two layers below surface). At a finite cluster size interval, there can be a coexistence of both the centered and quasisurface or asymmetric structures. As the transition from the center to the surface is expected to cause a blue shift, the coexistence of these two (or more) forms will result in an inhomogeneous line broadening in excitation and emission in accord with the experimental observations.

It is important to note that regardless of this structural transition the experimental pure radiative lifetime remained almost constant (being unaffected by it).

V. THEORETICAL CONSIDERATIONS

In our previous paper (paper I)[1] we have shown that many of the qualitative features of the effect of van der Waals complexation with rare-gas atoms on electronic absorption spectra and radiative lifetimes may be analyzed within a classical electrostatic model. We have also shown how a quantum mechanical treatment of these solvent effects reduces to the classical electrostatic result in the limit of first order perturbation theory. In our present discussion we shall distinguish between three situations with regards to the cluster size:

(1) The few atom clusters. This is the case that was theoretically treated in paper I, where each atom was taken as a point polarizable particle. Experimentally, for DCA, this situation corresponds to clusters smaller than about 20 Ar atoms where the frequency shift and radiative lifetime strongly depend on the cluster size.

(2) Many atom clusters whose size is much smaller than the wavelength of the radiation field at the molecular frequeny ω, i.e., $a \ll \lambda = 2\pi\omega/v$, where v is the speed of light in the cluster, $v = c/n$, and n being the refractive index.

(3) Large clusters, with size much larger than the wavelength of the radiation field. This is in fact the bulk limit.

In this section we review the results for case (1) and derive the results for the frequency shift and the radiative lifetime expected in case (2). These two cases cover all the experimental observations described in the previous section. Some interesting problems associated with the transition from case (2) to case (3) are discussed here but their detailed treatment is deferred to a future publication.

Few atom clusters. In paper I we have derived expressions for the modified radiative lifetime and the frequency shift for a molecule in a van der Waals cluster with a few rare-gas atoms. The molecule was represented by a Drude oscillator characterized by the bare molecular frequency ω_0, by a damping rate $\Gamma_R^{(f)}$ corresponding to the radiative damping rate of the free molecule and by a polarizability α which is related to the free radiative decay rate by

$$\alpha = \frac{3}{2}\frac{\Gamma_R^{(f)}}{\omega_0}\left(\frac{c}{\omega_0}\right)^3 . \tag{1}$$

The Drude oscillator represents the oscillating transition dipole μ. In the classical Drude picture it induces oscillating dipoles in the neighboring polarizable atoms. The modified radiative decay rate Γ_R is related to the total (molecular plus atomic) dipole in the system μ^{tot}

$$\Gamma_R = \left(\frac{\omega}{\omega_0}\right)^3 \frac{|\mu^{\text{tot}}|^2}{|\mu|^2}\Gamma_R^{(f)} , \tag{2}$$

where ω is the shifted molecular frequency. The frequency shift $\Delta\omega = \omega - \omega_0$ is obtained in terms of the ratio between the reaction field E_r at the molecule and the molecular dipole μ (E_r is the field due to the induced dipoles on the atoms)

$$\frac{\Delta\omega}{\omega_0} = -\frac{\alpha}{2\mu}\,\text{Re}(E_r) . \tag{3}$$

Note that since this E_r is linear in μ, this ratio does not depend on μ.

In paper I we have used these expressions in order to rationalize the observation that the radiative lifetime of the clustered molecule is longer than that of the free molecule. With the more detailed data available to us now, it is of interest to examine the theory in more detail. In view of the highly simplified model and of the classical approach used for the theoretical calculation, we should not expect quantitative agreement between theory and experiment. However we should be able to identify the important parameters of the problem and get a feeling for what this simplistic model can do on the quantitative level.

Equations (1)–(3) are strictly valid only for a molecule represented by a two level system and when the optical transition is far from saturation. There are many situations when such a description is sufficient even for large molecules, e.g., for a linear optical process near a molecular resonance. In particular, the relation (1) between $\Gamma_R^{(f)}$ and α arises from the two level (1 and 2 say) expression for the polarizability $\alpha = 2|\mu_{12}|^2(E_2 - E_1)$, where μ_{12} is the corresponding transition dipole matrix element. For a general many level system the polarizability is given as a sum over many terms like this. This is manifested, for example, by the different polarizabilities that can be associated with different electronic states. For example, the polarizabilities in the first excited singlet state of anthracene and of 9, 10-dimethylanthracene are 55 and 65 Å^3 (respectively) larger than in the ground states of the corresponding molecules.[18] Equation (1) cannot, therefore, be used in Eq. (3) for such systems. Instead, in the calculations reported below, we have used a general dispersion-type expression for the frequency shift: $\Delta\omega = C\Sigma\alpha_A/R_A^6$ where the sum is over all the atoms, R_A are the distances between the centers of the atoms and of the molecular dipole, α_A are the atomic polarizabilities and C is a constant which is determined by requiring that the shift calculated for the DCA. $(Ar)_1$ complex (see below for geometrical considerations) yields the experimentally obtained frequency shift for this complex. Physically, C corresponds to the difference in stabilization energy between the molecular ground and excited states upon binding the Ar.

We note in passing that the discussion above does not imply that Eq. (1) is useless for such molecules. The polarizability defined by Eq. (1) may be viewed as a "transition dipole polarizability" between two given states for an incident field at resonance with the corresponding transition, where Γ_R is the radiative width of the upper state associated with this transition.[19] It is in this way that we use Eq. (1) later [see Eq. (11)].

Another issue which should be addressed in any attempt to discuss quantitatively the correspondence between results obtained from this simple model calculation and the experimental results, is the distribution of the molecular dipole. In paper I we have represented the molecule by a point dipole $\boldsymbol{\mu}$ or by two charges of $\pm q$ separated by a distance l and is such that $q\mathbf{l}=\boldsymbol{\mu}$. [in general, one can model the molecule by a general charge distribution $\rho(\mathbf{r})$ satisfying $\boldsymbol{\mu} = \int d^3r\, \mathbf{r}\rho(\mathbf{r})$]. In paper I we have found that for l small relative to the atom-molecule distance, the effect of the finite dipole size was relatively small. The same conclusion is reached from the results obtained here with geometrical parameters corresponding to the DCA–rare-gas complexes. On the other hand, for a molecule like DCA with the electron density distributed essentially equally on the three aromatic rings, a representation of the molecular charge distribution by a single dipole at the molecular center is a gross oversimplification. While a complete distribution can be achieved only using the correct quantum mechanical molecular electronic structure, our classical model may be easily extended to more general charge distributions. In the lifetime calculations reported below we have compared results obtained from two models: one in which the molecule is represented by a single point dipole at the molecular center and the other in which the molecule is represented by six charges of equal magnitudes, two of opposite signs at the centers of each aromatic ring. Note that apart from its dependence on the positions of the rare-gas atoms, the lifetime calculation does not contain an adjustable parameter (except its very weak dependence on the shifted frequency ω). The corresponding evaluation of the frequency shift uses the expression

$$\Delta\omega = C\sum_A\sum_i \frac{\alpha_A}{R_{Ai}^6}, \tag{4}$$

where the sums over A and i are, respectively, over the atoms and over the ring centers (only one of the latter enters in the first model) and where the adjustable parameter C is determined as noted above. Note that this one single C is used for the complete set of calculations, and the same value of C was found to fit both models.

Next we provide the input data used in the following calculation. The atomic polarizabilities for Ar, Kr, and Xe are 1.64, 2.48, and 4.04 (in Å^3 units), respectively. The molecular plane is taken to be the ZY plane with the short and long molecular symmetry axes being along the Z and Y directions, respectively. The three ring centers are at $(x,y,z) = (0.,0.,0.)$, $(0., \pm 2.42,0.)$ (all distances are given in Å). The first rare-gas atom attaches to the molecule above the middle ring (along the X axis). The equilibrium distances between the center of this atom and the molecular center at the origin were taken (on the basis of semiempirical potential energy calculations) to be 3.42, 3.50, and 3.71 Å for Ar, Kr, and Xe, respectively. For complexes with up to eight Ar atoms the atomic positions used in our calculations are given in the following:

DCA·Ar$_1$: (3.42,0.,0.)
DCA·Ar$_2$: ($\pm$ 3.42,0.,0)
DCA·Ar$_3$: ($-$ 3.42,0.,0.), (3.42, $\pm$ 1.925,0.)
DCA·Ar$_4$: ($\pm$ 3.42,0.,0.), (3.42, $\pm$ 3.70,0.)
DCA·Ar$_5$: (3.42,0.,0.), (3.42, $\pm$ 3.70,0.), ($-$ 3.42, $\pm$ 1.925,0.)
DCA·Ar$_6$: ($\pm$ 3.42,0.,0.), ($\pm$ 3.42,3.70,0.) ($\pm$ 3.42, $-$ 3.70,0).
DCA·Ar$_7$: (3.42,0.,0.), ($\pm$ 3.42,3.70,0.), ($\pm$ 3.42, $-$ 3.70,0.), (0.,3.8,3.8)
DCA·Ar$_8$: (3.42,0.,0.), ($\pm$ 3.42,3.70,0.), ($\pm$ 3.42, $-$ 3.70,0.), (0., $\pm$ 3.8,3.8).

The positions taken for the first three Ar atoms are based on potential energy calculations for anthracene and tetracene.[20] For DCA·Ar$_4$ we have followed indications from these calculations that three of the four Ar atoms lie on the same side of the molecular plane. Due to uncertainties in the actual atomic positions we have taken the simplest choice of posi-

tioning these three atoms linearly along the Y axis. It is however quite possible that this atomic arrangement is not linear and that the atoms are staggered either within the ZY plane or within the XY plane. Our simpler choice which puts the atomic positions closer to the ring centers may be the reason why the results in Fig. 11 overestimate the increase in the radiative lifetime for the 4–6 complexes.

Finally, the structures of the 7 and 8 atoms clusters are guesses in which the 7th and 8th Ar atoms were taken to lie in the molecular plane, in the space between the chlorine atom and the ring. The choice of 3.8 Å for the corresponding distances is arbitrary but reasonable.

The two models for the molecular charge distribution in the lifetime calculation are: (a) A point dipole μ at (0.,0.,0.) in the Z direction, and (b) A pair of charges $\pm q$ centered at each of the three ring centers and separated by 1 Å along the Z direction. For model (b) we have also compared the results to those obtained by taking the charge separation in such a pair to be 0.1 Å (instead of 1 Å). This had only little effect on the calculated lifetimes. The adjustable constant C of Eq. (4) was found to be almost identical in the two models and a common value of $C = 3.3\times10^{-20}$ cm^2 was taken. Note that the calculated lifetime does not depend on the choices of μ or q.

Finally, the molecular parameters used in the calculation are $\omega_0 = 25\,947$ cm^{-1} for the 0–0 absorption peak, and $\Gamma_R^{(f)} = 2.28\times10^{-4}$ cm^{-1} for the free radiative decay width.

Using these input parameters we have calculated the frequency and the radiative lifetime shifts for the first eight DCA·AR$_n$ ($n = 1,\cdots8$) complexes (Fig. 11). This figure shows both the results of model (a) (circles) and of model (b) (squares) for the molecular charge distribution. Figures 12 and 13 show, respectively, the results of model (a) and (b) for the relative lifetime and frequency shifts of the

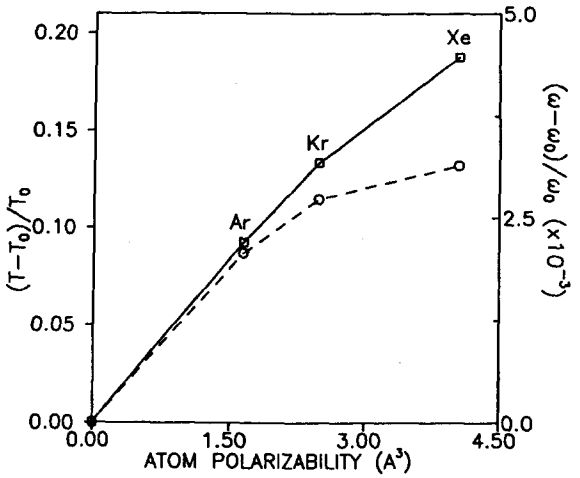

FIG. 12. Relative lifetime shifts (squares connected by a full line; right axis) and relative frequency shifts (circles connected by a dashed line; left axis) of DCA complexed with one Ar, Kr, or Xe atom, plotted against the atomic polarizability of the rare-gas atom. Model (a) for the molecular charge distribution was used in this calculation.

DCA·Ar, DCA·Kr, and DCA·Xe complexes. Comparing these results with the corresponding experimental results of Figs. 4 and 5, we see that a good semiquantitative agreement exists between the latter and between our simple model results, and that a considerable improvement in this agreement is achieved by going from model (a) that represents the molecule as a point dipole positioned at its center to model (b) which distributes the molecular charge over the three rings. It should be emphasized that no attempt was made to optimize the model results by changing the atomic positions or by using more details of the molecular charge distribution. One could get a better agreement with the experiment by

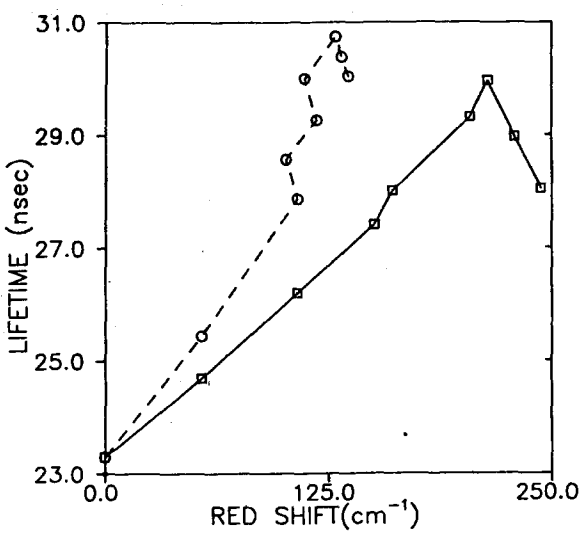

FIG. 11. Calculated radiative lifetime of several dichloroanthracene-Ar$_n$ ($n = 0,\cdots8$) complexes, plotted against the calculated frequency shifts. Circles connected by a dashed line are results of model (a) (see the text) while squares connected by a full line are results of model (b). See the text for the structures of the complexes.

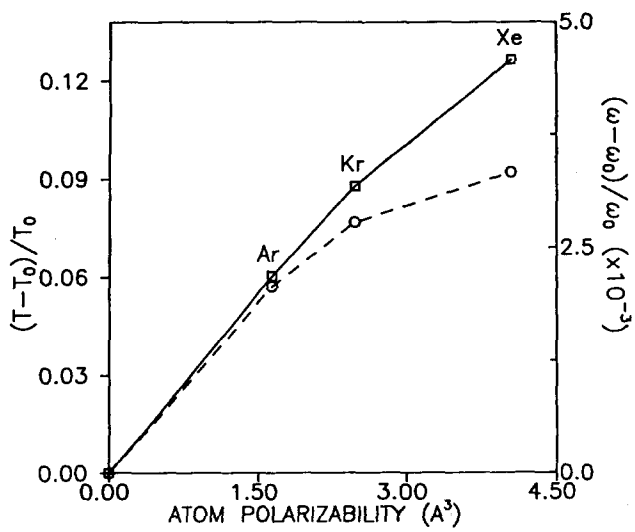

FIG. 13. Same as Fig. 12, with model (b) for the molecular charge distribution used in the calculation.

doing so, but the merit of doing it is questionable in view of the simplicity of the model.

Small many atom clusters. Consider now the intermediate cluster size case, where the cluster is large enough (relative to atomic size) so that it can be approximated as a small dielectric particle, but is still small relative to the radiation field wavelength. In this case we model the cluster as a dielectric sphere having the high frequency dielectric constant $\epsilon = n^2$ (n is the refractive index) of the corresponding bulk rare-gas solid. For Ar, Kr, and Xe these dielectric constants are 1.63, 1.88, and 2.19, respectively.

For the larger clusters now considered we resort to the simple representation of the molecule as a point dipole. The modified radiative lifetime may be obtained from Eq. (2), where $\mu^{\rm tot}$ is the total dipole of the molecule–sphere systems with μ representing the molecular (transition) dipole. The model is depicted in Fig. 14 in which the cluster is represented by a sphere of radius a and dielectric constant ϵ, and where the molecular dipole $\boldsymbol{\mu} = (\mu,\theta_0,0)$ is located at the point $\mathbf{r}_0 = (r_0,0,0)$ inside the sphere (i.e., $r_0 < a$).

The lifetime of a radiating dipole in a dielectric sphere can be calculated from generalizations of the Mie theory,[21] and general expressions are available.[22,23] Simpler results appropriate to small spheres ($a \ll \lambda$ where λ is the radiation wavelength *in the sphere*) may be derived as limiting cases of these expressions, or, more simply, by solving the corresponding classical electrostatics problem as follows: The field inside the sphere may be written (for $\mathbf{r} \neq \mathbf{r}_0$) as a solution to the Laplace equation [at point $\mathbf{r} = (r,\theta,\phi)$]

$$\Phi(r) = \frac{\boldsymbol{\mu}\cdot\mathbf{r} - \mathbf{r}_0}{\epsilon|\mathbf{r}-\mathbf{r}_0|^3} + \sum_{l=0}^{\infty}\sum_{m=-l}^{l} A_{lm} r^l Y_{lm}(\theta,\phi); \quad r \leqslant a\,, \tag{5}$$

where the first term on the right is the bare dipole potential. Outside the sphere the general solution of the Laplace equation is

$$\Phi(\mathbf{r}) = \sum_{l=0}^{\infty}\sum_{m=-l}^{l} B_{lm} r^{-l-1} Y_{lm}(\theta,\phi); \quad r \geqslant a\,. \tag{6}$$

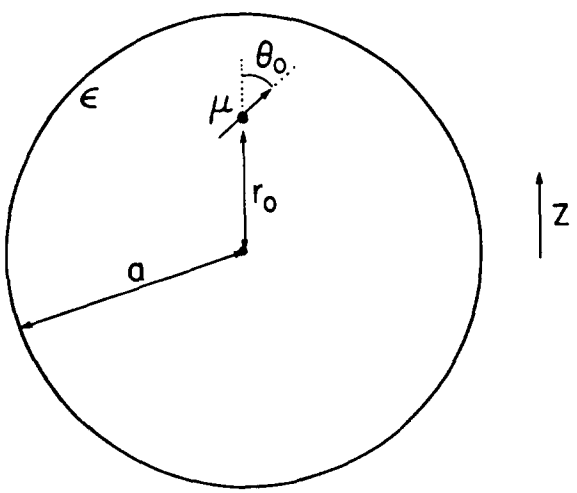

FIG. 14. A model for larger clusters: A point dipole (molecule) in a dielectric sphere (solvent).

The coefficients A and B are determined from the usual electrostatic boundary conditions, e.g., the continuity of the potential Φ and of the normal component of the displacement vector $\mathbf{D}$ at the sphere surface. The calculation is facilitated by expanding the $|\mathbf{r}-\mathbf{r}_0|^{-3}$ term in Eq. (5) in spherical functions. For $r > r_0$

$$\frac{\boldsymbol{\mu}\cdot\mathbf{r} - \mathbf{r}_0}{\epsilon|\mathbf{r}-\mathbf{r}_0|} = \frac{1}{\epsilon}\left\{\mu_z \sum_{l=0}^{\infty}\sqrt{\frac{4\pi}{2l+1}}\frac{l r_0^{l-1}}{r^{l+1}} Y_{l0}(\theta,\phi) - \mu_x \sum_{l=0}^{\infty}\sqrt{\frac{4\pi l(l+1)}{2l+1}}\frac{r_0^{l-1}}{2r^{l+1}} \times [Y_{l,1}(\theta,\phi) - Y_{l,-1}(\theta,\phi)]\right\} \tag{7}$$

with $\mu_x = \mu \sin\theta_0$ and $\mu_z = \mu\cos\theta_0$. For the potential outside the sphere we find $B_{lm} = 0$ for $|m| > 1$. Keeping only the dipolar $l = 1$ term we get

$$\Phi(\mathbf{r}) = \frac{3\boldsymbol{\mu}\cdot\mathbf{r}}{(\epsilon+2)r^3} \equiv \frac{\boldsymbol{\mu}^{\rm tot}\cdot\hat{\mathbf{r}}}{r^2}; \quad r \to \infty\,, \tag{8}$$

where $\hat{\mathbf{r}}$ is a unit vector in the $\mathbf{r}$ direction. Hence

$$\boldsymbol{\mu}^{\rm tot} = \frac{3}{(\epsilon+2)}\boldsymbol{\mu} \tag{9}$$

is the total dipole of the molecule–cluster system. Interestingly, this result is independent both of the sphere radius (in this limit where a is much smaller than the radiation wavelength) and of the location of the molecule in the sphere. Note that this feature is in accord with out conjecture (Sec. IV E) that the migration of the molecule to the cluster surface does not change its radiative lifetime. If we disregard the very small correction $(\omega/\omega_0)^3$, we get from Eq. (2)

$$\Gamma_R/\Gamma_R^{(f)} = [3/(\epsilon+2)]^2 \tag{10}$$

which for Ar yields about a 40% longer radiative lifetime, independent of the cluster size in this limit. The experimental results show saturation of the cluster effect on the fluorescence lifetime at about a 12% increase. The difference may be due, at least in part, to the fact that the effective dielectric constant of the cluster is smaller than its bulk value. The prediction for the corresponding saturation values for Kr and Xe are $\simeq$65% and 95%, respectively.

It is interesting to consider also the oscillator strength, namely the integrated absorption line shape of the clustered molecule. One may ask whether it is related to the modified radiative decay rate in the same way as the oscillator strength and the radiative lifetime of the free molecule. This in fact should be so, because the clustered molecule does behave as any other absorbing species, so to show it from our model calculation provides an important consistency check. To demonstrate this consider the Drude-like equation for the molecular transition dipole:

$$\ddot{\boldsymbol{\mu}} + \Gamma_R\dot{\boldsymbol{\mu}} + \omega^2\boldsymbol{\mu} = \omega^2\alpha\frac{3}{\epsilon+2}E_\mu\,. \tag{11}$$

Here $\mathbf{E}_\mu$ is the incident field in the $\boldsymbol{\mu}$ direction, Γ_R and ω are the actual radiative decay rate and frequency, and α is the transition dipole polarizability given by Eq. (1). The factor $3/(\epsilon+2)$ relates the incident field to the field inside the dielectric sphere. Multiplying Eq. (11) by $3/(\epsilon+2)$ and using Eq. (9) we get

$$\ddot{\boldsymbol{\mu}}^{\rm tot} + \Gamma_R \dot{\boldsymbol{\mu}}^{\rm tot} + \omega^2 \boldsymbol{\mu}^{\rm tot} = \omega^2 \alpha \left(\frac{3}{\epsilon+2}\right)^2 \mathbf{E}_\mu \,. \tag{12}$$

The absorption cross section associated with Eq. (12) is given by[24]

$$\sigma(\Omega) = \frac{1}{4}\left[\frac{2\pi c}{\omega}\right]^2 \Gamma_R^{(f)} \left(\frac{3}{\epsilon+2}\right)^2 \frac{\Gamma_R/2\pi}{(\Omega-\omega)^2 + (\Gamma_R/2)^2} \,. \tag{13}$$

This differs from the usual expression for the absorption cross section only by the appearance of the factor containing the sphere dielectric constant (note that for $\epsilon = 1$ this factor disappears). Using Eq. (10) we see that the absorption cross section takes the usual form with Γ_R replacing $\Gamma_R^{(f)}$, so the former will now replace the latter in the oscillator strength

$$\int d\Omega\, \sigma(\Omega) = \frac{1}{4}\left[\frac{2\pi c}{\omega}\right]^2 \Gamma_R \tag{14}$$

which concludes our proof.

Next consider the frequency shift for this case. Eq. (3) may again be used where E_r is the reaction field at the molecule due to the polarization of the sphere by the molecular dipole μ. Solving the electrostatic problem defined by Eqs. (5)–(7) we get the A coefficients of Eq. (5). Hence the reaction potential $\Sigma A_{lm} r^l Y_{lm}(\theta,\phi)$ inside the sphere. From this we get the reaction field in the direction of the molecular dipole in the form

$$E_R = -\frac{\mu}{\epsilon} \sum_{l=0}^{\infty} \left[l^2(l+1)\cos^2\theta + \frac{1}{2} l(l+1)^2 \sin^2\theta \right] \times \frac{r_0^{2(l-1)}}{a^{2l+1}} \frac{\epsilon-1}{\epsilon l + l + 1} \,. \tag{15}$$

Using this in Eq. (3) yields the frequency shift *relative to an homogeneous environment with dielectric function* ϵ. In particular, for a molecule located in the middle of the spherical cluster ($r_0 = 0$) only the $l = 1$ term contributes, and we get

$$E_R = -\frac{2\mu}{\epsilon a^3} \frac{\epsilon-1}{\epsilon+2} \,. \tag{16}$$

This with Eq. (3) yields

$$\frac{\Delta\omega}{\omega} = \frac{\alpha}{\epsilon a^3} \frac{\epsilon-1}{\epsilon+2} \,. \tag{17}$$

Neglecting the polarizability of the ground state DCA and taking $\alpha \cong 60$ Å^3 for the excited DCA, and using $\epsilon = 1.63$ (Ar) we find within this continuum dielectric model that increasing the cluster size from $a = 20$ Å to ∞ causes an additional frequency shift of less than 10^{-4} $\omega \cong 25$ cm^{-1}, namely 95% of the observed shift develops before the cluster reaches this size, which is in accordance with the experimental observation. The trend to saturation of the frequency shift will be even faster if the molecule tends to sit just beneath the cluster surface because then additional cluster atoms will add themselves at the further (from the molecule) end of the cluster.

Finally, consider the bulk limit. Both theory and experiment agree that the lifetime of a molecule embedded in a dielectric solvent is shorter than that of the free molecule.[25] While no experimental data are available for DCA in a rare gas matrix, the fluorescence lifetime in cyclohexane ($\epsilon = 2.04$) is $\cong 15$ ns, about half that of the free molecule. This implies that when the cluster size increases beyond the radiation field wavelength, the radiative lifetime should decrease substantially. At the same time the relation between the oscillator strength (integrated absorption) and the radiative lifetime should change from its vacuum form which is independent of the solvent dielectric function (as we saw above this form holds also for small clusters which to the source and the detector appear as molecules) to its solvent form which depends on it. The length range in which this transition occurs should be related either to the radiation wavelength λ or to a length defined by the speed of light v (in the cluster) and the fluorescence lifetime τ. $v\tau$ however is of the order of 10 cm which seems too large to be relevant in this context. It would be interesting to study this size evolution effect both experimentally and theoretically.

VI. CONCLUSIONS

In this paper we have presented experimental and theoretical results that elucidate the effect of a small cluster environment on the optical properties of an embedded molecule. The molecular absorption line shape and the radiative emission lifetime are affected in a pronounced way which strongly depends on the cluster size and geometry for the few atom clusters, and become quite insensitive for intermediate size spherical clusters whose size is much smaller than the radiative wavelength. At such sizes the absorption red shift is practically fully developed, however the radiative lifetime is larger than that of the free molecule (and, remarkably, independent of the molecular location within the cluster) while the corresponding lifetime in the bulk solvent is expected to be shorter. Thus, a further transition in the lifetime behavior is expected when the cluster size exceeds the radiation wavelength.

ACKNOWLEDGMENTS

This reasearch was supported in part by the Commission for Basic Research of the Israel Academy of Science (to A. A. and to A. N.) by the U.S.–Israel Binational Science Foundation (to A. N.). Helpful discussion with L. Brus, M. McClain, A. Tramer, and E. Weitz are gratefully acknowledged.

[1] N. Liver, A. Nitzan, A. Amirav, and J. Jortner, J. Chem. Phys. **88**, 3516 (1988).
[2] M. Sonnenschein, A. Amirav, and J. Jortner, J. Phys. Chem. **88**, 4214 (1984).
[3] E. C. Lim, J. D. Laposa, and J. M. H. Yu, J. Mol. Spectrosc. **19**, 412 (1966).
[4] A. Amirav, C. Horwitz, and J. Jortner, J. Chem. Phys. **88**, 3092 (1988).
[5] A. Tramer (private communications).
[6] G. D. Gillispie and E. C. Lim, Chem. Phys. Lett. **63**, 193 (1979).
[7] A. Amirav, U. Even, and J. Jortner, Chem. Phys. **51**, 31 (1980).
[8] A. Amirav, U. Even, and J. Jortner, J. Chem. Phys. **75**, 2489 (1981).
[9] A. Amirav, U. Even, and J. Jortner, J. Chem. Phys. **86**, 3345 (1982).
[10] A. Amirav, M. Sonnenschein, and J. Jortner, Chem. Phys. **88**, 199 (1984).
[11] U. Even and J. Jortner, J. Chem. Phys. **78**, 3445 (1983).
[12] A. Amirav, U. Even, and J. Jortner, Chem. Phys. Lett. **67**, 9 (1979).
[13] U. Even, N. Ben-Horin, and J. Jortner, Chem. Phys. Lett. **156**, 138 (1989) and Phys. Rev. Lett. **62**, 140 (1989).
[14] Isadore B. Berlman, in *Handbook of Fluorescence Spectra of Aromatic Molecules* (Academic, New York, 1965).

[15]A. Amirav, U. Even, and J. Jortner, J. Chem. Phys. **75**, 3770 (1981).
[16](a) M. Bixon and J. Jortner, J. Chem. Phys.**91**, 1631 (1989); (b) T. L. Back and R. S. Berry, J. Chem. Phys. **88**, 3910 (1988), and references therein.
[17](a) T. E. Gough, D. G. Knight, and G. Scoles, Chem. Phys. Lett. **97**, 155 (1983); (b) J. C. Shelley and R. J. Le Roy, Chem. Phys. Lett. **152**, 14 (1988).
[18]A. Davidsson and L. B. A. Johanson, Mol. Phys. **57**, 295 (1986).
[19]J. Gersten and A. Nitzan, J. Chem. Phys. **75**, 1139 (1981).
[20]M. J. Ondrechen, Z. Berkovitch-Yellin, and J. Jortner, J. Am. Chem. Soc. **103**, 6586 (1981).
[21]B. Mie, Ann. Phys. (Leipzig) **25**, 377 (1908). For modern reviews see, M. Born and E. Wolf, *Principle of Optics* (Pergamon, Oxford, 1975); M. Kerhen, *The Scattering of Light and Other Electromagnetic Radiation* (Academy, New York, 1969).
[22]H. Chew, J. Chem. Phys. **87**, 1355 (1987).
[23]Y. S. Kim, P. T. Leung, and T. F. George, Surf. Sci., **195**, 1 (1988).
[24]A. Nitzan and L. E. Brus, J. Chem. Phys. **75**, 2205 (1981).
[25]See, for example, S. Hiryama, and D. Phillips, J. Photochemistry **12**, 139 (1980).